Temporally and spatially resolved imaging of laser-nucleated bubble cloud sonoluminescence

Jonathan R. Sukovich, Ashwin Sampathkumar, Phillip A. Anderson, and R. Glynn Holt
Department of Mechanical Engineering, Boston University, Boston, Massachusetts 02215, USA

Yuri A. Pishchalnikov and D. Felipe Gaitan
Impulse Devices, Inc., Grass Valley, California 95945, USA
(Received 20 December 2011; published 17 May 2012)

Imaging techniques have been used to capture the temporal and spatial evolution of light emissions from collapsing bubble clouds at high static pressures. Emission events lasting up to 70 ns with peak diameters nearing 1 mm have been observed. Observations of the cloud evolution before and after emission events have been made. Photomultiplier tube monitoring has been employed in conjunction with imaging to study the temporal characteristics of light emission.

DOI: 10.1103/PhysRevE.85.056605 PACS number(s): 43.35.Hl

I. INTRODUCTION

Single-bubble sonoluminescence (SBSL), the process by which a light-emitting gas bubble is trapped in a resonant sound field, has been a topic of great interest since it was observed by Gaitan *et al.* [1]. Of particular interest have been the temperatures and pressures reached in the bubble's center and the mechanisms by which light is generated. To that end, the duration and size of SBSL events have been studied extensively to provide physical constraints on the mechanisms responsible for light emission. Observations have shown that the duration of SBSL light emission is typically on the order of 30–300 ps [2], with light-emitting regions having typical diameters of less than 3 μm [3]. Multibubble sonoluminescence, in contrast, is typically less well confined to particular regions of space (and time) [4] and past studies have used other metrics such as spectroscopy [5] to describe the characteristics of the events.

II. EXPERIMENTAL SETUP

In this paper we present time-resolved images of light emission and the cloud evolution leading up to and following the production of light, resulting from the collapse of compact clouds of laser nucleated bubbles. Events in this paper are defined as the collapse phase of bubble clouds and resulting light emissions during each cycle. Bubble clouds were nucleated in an array pattern using a pulsed Nd:YAG laser shone through a series of phase gratings and focused into the center of a high-pressure spherical resonator (Impulse Devices, Inc.) (Fig. 1) (for a more detailed experimental setup see Ref. [6]). Experiments were carried out in water at ambient pressures of up to 30 MPa and acoustic pressures of up to 35 MPa. Water used in the experiments was filtered to 0.2 μm and was degassed by equilibration with air at 120 Torr. Time-resolved images of individual events were taken using a high-speed camera (SIM-X8) with exposure and interframe times individually optimized for the experiment. The light emissions of the time-resolved events were monitored using a photomultiplier tube (PMT) (Photonis XP2262B) with a 1-kV bias voltage. A 532-nm Raman Notch Filter was placed in front of the PMT to avoid saturation damage to the PMT when the laser was fired. Images of the cloud evolution with simultaneous light emissions were backlit using a white cw light source. Photomultiplier tube monitoring was not utilized in the simultaneous backlit experiments. (The images in Figs. 2 and 4 were cropped down from their original form for ease of analysis and viewing.)

III. RESULTS

Time-resolved images of individual emission events (see Fig. 2) showed explosive growth of the central emission region, with front velocities up to approximately 30 km/s. It should be noted that in Fig. 2 the bright, compact central emission region saturated the CCD elements in frames 2–5, though we do not believe the saturation of individual pixels in the brightest regions had an appreciable effect on adjacent pixels and hence the size of the emission region measured. It was observed that the formation and growth of emissions regions were varied, but followed two main paths of evolution. Strong events tended to grow from a single initial emission region into large, uniform, regions with diameters reaching 1 mm. Weak events tended to grow from multiple small emitting regions into moderately sized consolidated but nonuniform regions. These consolidated regions were observed to reach diameters of up to 300 μm with separations of up to 500 μm.

The decay of emission regions also showed interesting features depending on the mode of formation and overall size. It appears that large singular emission regions tended to break apart into smaller emission regions before fading out entirely. Smaller individual events were observed to maintain uniformity during decay and eventually blink out. The consolidated but nonuniform regions observed in the weak events were observed to decay independently and tended to follow the decay pattern of the smaller individual events. This difference in spatial decay patterns between the strong and weak event suggests that for significantly large events an internal structure develops that modifies the decay of the region, whereas smaller events seem less susceptible to whatever perturbations may lead to the development of internal structures.

Photomultiplier tube monitoring of the evolution of events yielded other insights. Many events were shown to have multiple peaks in the emission curve for a single event (Fig. 3). The separation times between peaks observed in these multipeak

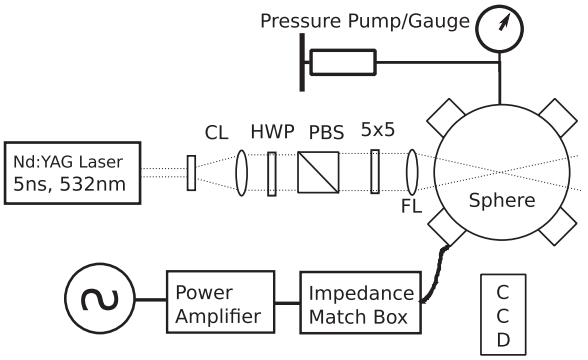

FIG. 1. Schematic of the experimental setup for imaging experiments: CL, collimation lenses used to expand the beam waist from 1 to 25 mm; HWP, half wave plate used to adjust the polarization angle of the light exiting the laser; PBS, polarizing beam splitter used in combination with the half wave plate to adjust the downstream laser energy, 5 × 5, phase grating responsible for generating the 5 × 5 grid pattern of laser beams; FL, 125-mm focal length lens used to focus the laser into the center of the sphere.

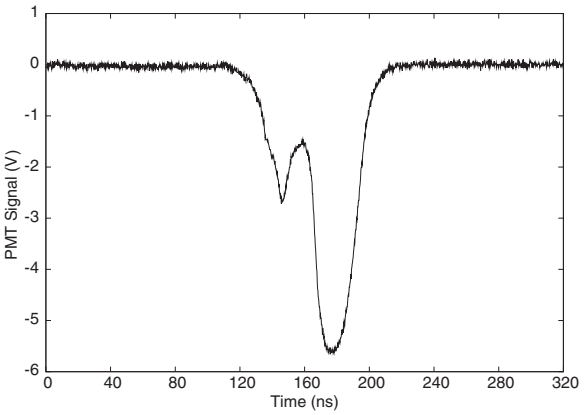

FIG. 3. Photomultiplier tube signal of a single event showing multiple peaks.

events were typically on the order of a few tens of nanoseconds, but were occasionally observed to be larger. Similar events have been observed in transient cavitation experiments at these elevated pressures [7]. This likely suggests nonuniformities in either the pressure or bubble distribution in the collapse region or that the conditions requisite for emissions are probabilistic in nature and so may occur at any point in space or time in the region so long as conditions are above some threshold value. Another very plausible explanation is that there are two or more simultaneous clusters, which, owing to differences in size, collapse at different times.

An analysis of events over multiple cycles yielded further insight. Figure 4 shows spatial overlays of images of single events over multiple acoustic cycles. It can be seen that the events of cycles 6, 7, 10, and 11 are fairly localized, with events confined to a region of space a little larger than a millimeter. Events from cycles 8, 9, 12, and 13 are more scattered and generally weaker than localized events preceding them. The spatial variation in the cycles following the localized events is likely due to asymmetries during the collapse that leave seed nuclei for the next cycle randomly dispersed in the collapse region. The clustering observed in cycles 6, 7, 10, and 11, however, is the result of the system entering a mode-locked state where outgoing shock waves from one collapse event return to the center of the system four cycles later and nucleate a new cloud in their wake [6,7].

Simultaneous backlit images (Fig. 5) offered further insights into the cloud evolution immediately before and after emissions events. Emission events typically occurred when the apparent cloud radius fell below 500 μm. Previous work [6] has shown that cloud radii approach a maximum expansion of 3 mm for the pressures and nucleation schemes described above. This observation yields a lower bound for the volume compression ratio resulting in light emission of approximately 250. This is orders of magnitude lower than the volume compression ratios observed for SBSL; however, minimum radii for SBSL have generally only been inferred

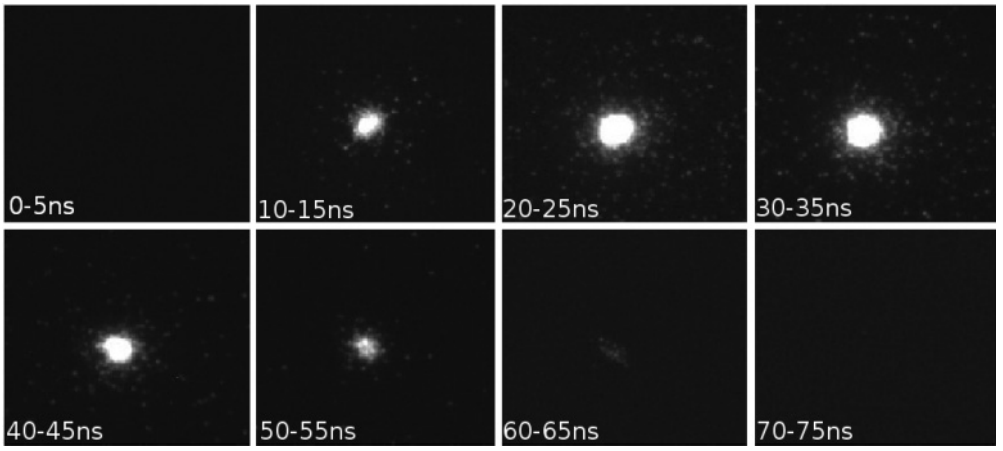

FIG. 2. Time-resolved images of a light emission event with a (5 × 5)-mm field of view. This experiment was carried out at an ambient pressure of 30 MPa with a peak acoustic pressure of 35 MPa. The laser was fired 1 μs before the peak negative phase of the acoustics to nucleate the cloud and the first image began 20 ns before the peak positive phase of the acoustics. The image series spanned 75 ns with each frame having an exposure time of 5 ns with another 5 ns between frames. Frames 1–4 progress from left to right on the top row of the image series, followed in a similar fashion by frames 5–8 on the bottom row.

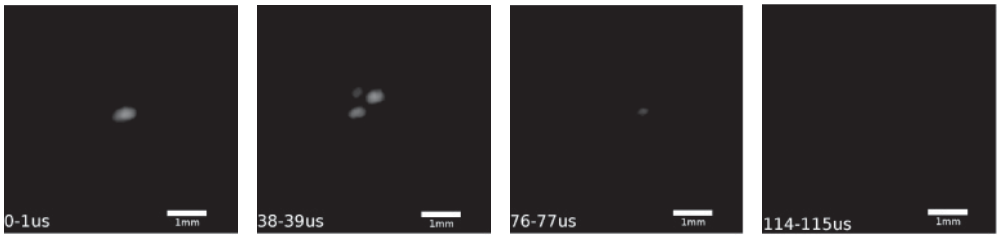

(a)Cycle 6 (b)Cycle 7 (c)Cycle 8 (d)Cycle 9

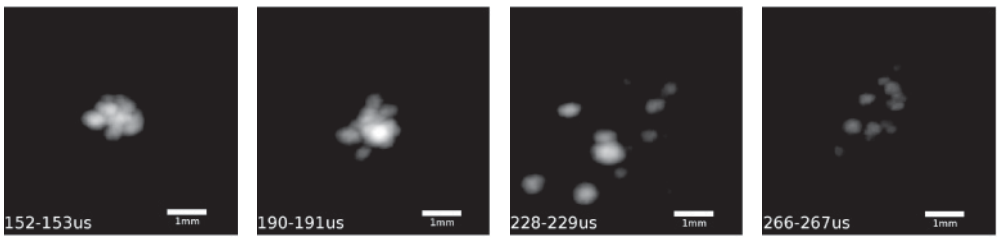

(e)Cycle 10 (f)Cycle 11 (g)Cycle 12 (h)Cycle 13

FIG. 4. Overlay plots of the evolution of events from 36 eight-cycle image sequences. This experiment was carried out at an ambient pressure of 17 MPa with a peak acoustic pressure of 22 MPa. Exposure times were set to 1 μs with each image starting 500 ns before the peak positive pressure of each listed cycle, with cycles lasting 38 μs. The laser was fired once at cycle 0, 1 μs before the peak negative phase of the acoustics. These images were made by stacking frames from 36 sets of images of events over 8 acoustic cycles on top of one another. This involved going pixel by pixel through each of the 36 frames per cycle and comparing the brightness of that pixel in each frame and then assigning the new pixel the brightest value observed in the 36 frames. This ensured that each image would show peak brightness as well as the spatial distribution of SL events from cycle to cycle without diminishing events that were not centrally located as simple averaging would have.

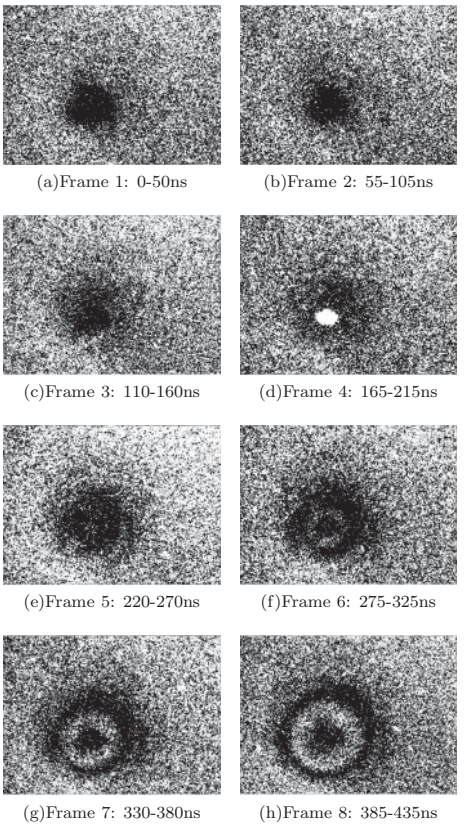

(a)Frame 1: 0-50ns (b)Frame 2: 55-105ns

(c)Frame 3: 110-160ns (d)Frame 4: 165-215ns

(e)Frame 5: 220-270ns (f)Frame 6: 275-325ns

(g)Frame 7: 330-380ns (h)Frame 8: 385-435ns

FIG. 5. Backlit image of a light emission event with a (4 × 3)-mm field of view. The image series spanned 435 ns with frame exposure times of 50 and 5 ns between each frame. Frames 1–3 show the final stages of the cloud collapse, frame 4 shows the light emission event, and frames 5–8 show the development of a shock wave from the collapse.

from simulation [8,9]. The spatial distribution of events was observed to be scattered about the center of the collapse region, with the highest density of emission events occurring within 35–70 μm from the center. This is further evidence of either nonuniformities in the region or a threshold effect. Backlit images also revealed that the first detectable shock waves are observed approximately 50–100 ns after the light emissions fade out with a radius of approximately 0.45 mm and a velocity of just under 6500 m/s. Figure 6 shows a condensed plot of the radius versus time for a cloud during the final stages of collapse, the radius of the SL event over its duration, and the radius of the shock immediately following the collapse.

The effects of static pressure on emission events were also measured. The total light output from emission events, as measured by the PMT, was observed to increase with

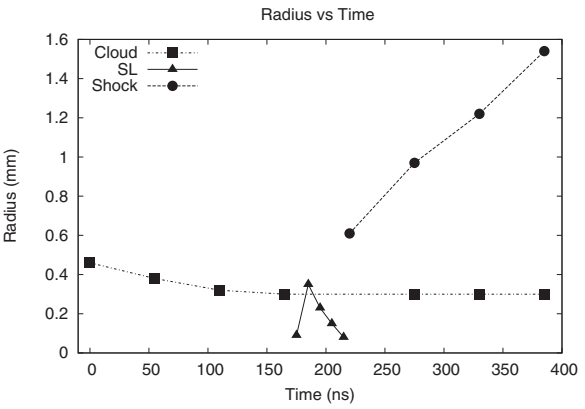

FIG. 6. Radius vs time plot showing the cloud, sonoluminescence (SL), and shock radius for a typical event. The uncertainties in the values presented are ±10 μm.

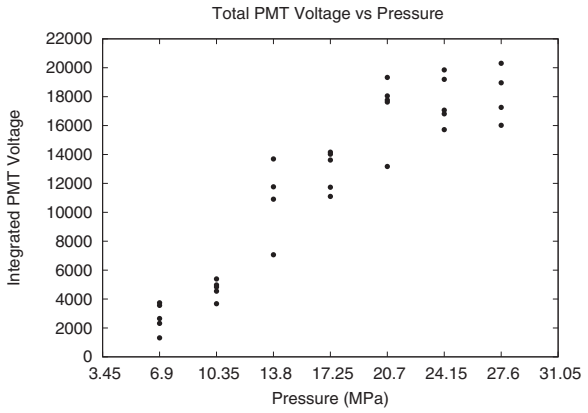

FIG. 7. Integrated PMT signal vs pressure data from five experiments at each pressure from 6.9 to 27.6 MPa. Each data point represents the integration of the PMT signal from the nucleation of the first bubble cloud to the last observable event in the run.

increasing static pressure (Fig. 7). Similar results have been observed in experiments relating the static pressure to the collapse strength of bubble clouds [7,10]. The number of observable events and the size and total light emission from events also increased with pressure. The increase in light output seems to slow down at higher pressures. These results corroborate results for spontaneously nucleated SL in spherical resonators reported in Ref. [7]. The PMT results also show increased scatter in total light emissions at higher pressures, which may be the result of the nonuniform or probabilistic nature of the events as described above.

IV. CONCLUSION

In conclusion, we have shown an effective technique for imaging the collapse and light emissions from large, violently collapsing, bubble clusters in water. We have seen events lasting many orders of magnitude longer than those of previous studies. Similarly, we have measured light-emission events reaching diameters on the order of 1 mm. We have shown that peak emissions and collapse strength increase with increasing static pressure and that emissions tend to occur when the volume compression ratio of the cloud reaches 250:1. Observations revealed that emissions are not necessarily localized to the center of the collapse region, but can occur throughout. Moreover, in a given collapse event, multiple emission regions can develop simultaneously to produce light.

ACKNOWLEDGMENT

This work was funded by Impulse Devices Inc.

[1] D. F. Gaitan, L. A. Crum, C. C. Church, and R. A. Roy, J. Acoust. Soc. Am. **91**, 3166 (1992).
[2] B. Gompf, R. Gunther, G. Nick, R. Pecha, and W. Eisenmenger, Phys. Rev. Lett. **79**, 1405 (1997).
[3] M. J. Moran, R. E. Haigh, M. E. Lowry, D. R. Sweider, G. R. Abel, J. T. Carlson, S. D. Lewia, A. A. Atchley, D. F. Gaitan, and X. K. Maruyama, Nucl. Instrum. Methods Phys. Res. Sect. B **96**, 651 (1995).
[4] W. Lauterborn, T. Kurz, R. Geisler, D. Schanz, and O. Lindau, Ultrason. Sonochem. **14**, 484 (2007).
[5] R. A. Hiller, S. J. Putterman, and K. R. Weninger, Phys. Rev. Lett. **80**, 1090 (1998).
[6] P. A. Anderson, A. Sampathkumar, T. W. Murray, D. F. Gaitan, and R. G. Holt, J. Acoust. Soc. Am. **130**, 3389 (2011).
[7] D. F. Gaitan, R. A. Tessien, R. A. Hiller, J. Gutierrez, C. Scott, H. Tardif, B. Callahan, T. J. Matula, L. A. Crum, R. G. Holt, C. C. Church, and J. L. Raymond, J. Acoust. Soc. Am. **127**, 3456 (2010).
[8] D. F. Gaitan and R. G. Holt, Phys. Rev. E **59**, 5495 (1999).
[9] S. Hilgenfeldt, M. P. Brenner, S. Grossman, and D. Lohse, J. Fluid Mech. **365**, 171 (1998).
[10] K. B. Bader, Ph.D. thesis, University of Mississippi, 2011.